

Non-centrosymmetric Superconductivity and Antiferromagnetic Order: Microscopic discussion of CePt₃Si

Youichi YANASE^{1,2*} and Manfred SIGRIST^{2,3}

¹ Department of Physics, University of Tokyo, Tokyo 113-0033, Japan

² Theoretische Physik, ETH-Honggerberg, 8093 Zurich, Switzerland

³ Department of Physics, Kyoto University, Kyoto 606-8502, Japan

(Received Today 2006)

The influence of antiferromagnetic order on the superconductivity in the non-centrosymmetric heavy fermion compound CePt₃Si and related materials is discussed. Based on our RPA analysis for the extended Hubbard model two phases could be stabilized by a spin fluctuation induced pairing, with either dominantly *p*-wave or *d*-wave symmetry. The antiferromagnetic order plays an essential role for the low-energy physics, in particular, for the appearance of line nodes in the gap and the enhancement of spin susceptibility below T_c . Various properties and possible phase diagrams under pressure are analyzed. The present experimental situation suggests that the *p*-wave phase is most likely realized in CePt₃Si.

KEYWORDS: Superconductivity without inversion center; antiferromagnetic superconductor

Since the discovery of superconductivity in the non-centrosymmetric heavy Fermion compound CePt₃Si,¹ superconductivity in materials without inversion center has been attracting growing interest. Many new non-centrosymmetric superconductors with unusual properties have been identified among heavy fermion systems such as UIr,² CeRhSi₃,³ CeIrSi₃,⁴ CeCoGe₃⁵ and others like Li₂Pd_xPt_{3-x}B,⁶ and KOs₂O₆.⁷ One immediate consequence of non-centrosymmetry is the necessity for a revised classification scheme of Cooper pairing states, as parity is not available as a distinguishing symmetry. The pairing states is considered as mixtures of states with different parity imposed by the presence of antisymmetric spin-orbit coupling (ASOC).⁸ Recent theoretical studies let to the proposal of various intriguing properties of such a superconductor.⁸⁻¹⁴

In the past the relation between superconductivity and magnetism has been one of the aspects of major interest in heavy fermion systems. Interestingly, all presently known non-centrosymmetric heavy Fermion superconductors, i.e. CePt₃Si, UIr, CeRhSi₃, CeIrSi₃ and CeCoGe₃, coexist with the magnetism. Although magnetism affects the electronic state profoundly, most of the theoretical studies except for Refs. 14 and 15 neglected this aspect so far. The aim of the present study is to elucidate how the magnetism influences the superconducting (SC) phase and how it may be involved in deciding the pairing symmetry in CePt₃Si. Among the non-centrosymmetric heavy fermion superconductors, CePt₃Si has been investigated in most detail because the superconductivity occurs at ambient pressure.¹ Although we focus here on CePt₃Si, we believe that some of our results are qualitatively valid for the other compounds too.

In CePt₃Si superconductivity with $T_c = 0.75\text{K}$ appears in the antiferromagnetic (AFM) state with Neel temperature $T_N = 2.2\text{K}$.¹ Neutron scattering measurements characterize the AFM order with an ordering wave vector $Q = (0, 0, \pi)$ and magnetic moments in

the *ab*-plane of the tetragonal crystal lattice.¹⁶ The nature of the SC phase has been characterized by several experiments. The low-temperature properties of the thermal conductivity,¹⁷ superfluid density¹⁸ and specific heat¹⁹ indicate line nodes in the gap, while the coherence peak in NMR $1/T_1T$ is a feature expected rather for a conventional superconductor.²⁰ The upper critical field $H_{c2} \sim 4\text{T}$ exceeds the standard paramagnetic limit,¹ which seems to be consistent with the Knight shift data displaying no decrease of the spin susceptibility below T_c for any field direction.^{21,22} The combination of all these features is incompatible with the usual pairing states such as the *s*-wave, *p*-wave or *d*-wave state, and calls for an extension of the standard working scheme.

For the following study of superconductivity in CePt₃Si, we introduce the single-orbital Hubbard model including AFM order and ASOC, expressed as

$$H = \sum_{\vec{k}, s} \varepsilon(\vec{k}) c_{\vec{k}, s}^\dagger c_{\vec{k}, s} + \alpha \sum_{\vec{k}, s, s'} \vec{g}(\vec{k}) \cdot \vec{\sigma}_{ss'} c_{\vec{k}, s}^\dagger c_{\vec{k}, s'} - \sum_{\vec{k}, s, s'} \vec{h}_Q \cdot \vec{\sigma}_{ss'} c_{\vec{k}+\vec{Q}, s}^\dagger c_{\vec{k}, s'} + U \sum_i n_{i,\uparrow} n_{i,\downarrow}. \quad (1)$$

We consider a simple tetragonal lattice and assume the dispersion relation as,

$$\begin{aligned} \varepsilon(\vec{k}) = & 2t_1(\cos k_x + \cos k_y) + 4t_2 \cos k_x \cos k_y \\ & + 2t_3(\cos 2k_x + \cos 2k_y) + [2t_4 + 4t_5(\cos k_x + \cos k_y) \\ & + 4t_6(\cos 2k_x + \cos 2k_y)] \cos k_z + 2t_7 \cos 2k_z - \mu, \quad (2) \end{aligned}$$

which reproduces the so-called β -band of CePt₃Si as obtained from band structure calculations without taking AFM order into account.²³⁻²⁵ The β -band has a substantial Ce *4f*-electron character²⁵ and the largest density of states (DOS), namely 70% of the total DOS.²³ We determine the chemical potential μ so that the electron density per site is n and the parameters as $(t_1, t_2, t_3, t_4, t_5, t_6, t_7, n) = (1, -0.15, -0.5, -0.3, -0.1, -0.09, -0.2, 1.75)$ defining t_1 as the unit energy.

The second term in eq. (1) describes the ASOC due to the lack of inversion symmetry. In case of CePt₃Si the g -vector has the Rashba type structure.^{9,10} Although the detailed momentum dependence of the g -vector is not easily obtained from band structure calculations, it can reasonably be expressed in terms of velocities $v_{x,y}(\vec{k}) = \partial \varepsilon(\vec{k}) / \partial k_{x,y} : \vec{g}(\vec{k}) = (-v_y(\vec{k}), v_x(\vec{k}), 0) / \bar{v}$. We normalize \vec{g} by the average velocity \bar{v} [$\bar{v}^2 = \frac{1}{N} \sum_k v_x(\vec{k})^2 + v_y(\vec{k})^2$]. This form reproduces the correct symmetry and periodicity of the $\vec{g}(\vec{k})$ within the Brillouin zone. We choose the coupling constant $\alpha = 0.3$ so that a band splitting due to ASOC is consistent with the band structure calculations.²³ Figure 1 shows the Fermi surfaces in our model.

The AFM order enters in our model through the staggered field \vec{h}_Q without discussing its microscopic origin. The phase diagram under pressure implies that the AFM order is mainly carried by localized Ce $4f$ -electrons which have a character different from the SC quasiparticles. The SC T_c is little affected by the AFM order which vanishes at $P \sim 0.6\text{GPa}$ ²⁶ in contrast to the other Ce-based superconductor.²⁷ The experimentally determined order corresponds to \vec{h}_Q pointing along the x -direction with a wave vector $\vec{Q} = (0, 0, \pi)$.¹⁶ For the magnitude we choose $h_Q \ll W$ where W is the band width since the observed moment $\sim 0.16\mu_B$ is considerably less than the full moment of the Ce-ion.¹⁶ We do not touch the complex heavy Fermion aspect, i.e. the hybridization of the conduction electrons with the Ce $4f$ -electrons forming the strongly renormalized quasiparticles. However we consider the Hubbard model as a valid effective model to describe the low-energy quasiparticles.²⁸

The undressed Greens function for $U = 0$ has the matrix form, $\hat{G}(\vec{k}, i\omega_n) = (i\omega_n \hat{1} - \hat{H}(\vec{k}))^{-1}$, where

$$\hat{G}(\vec{k}, i\omega_n) = \begin{pmatrix} \hat{G}^1(\vec{k}, i\omega_n) & \hat{G}^2(\vec{k}, i\omega_n) \\ \hat{G}^2(\vec{k}_+, i\omega_n) & \hat{G}^1(\vec{k}_+, i\omega_n) \end{pmatrix}, \quad (3)$$

$$\hat{H}(\vec{k}) = \begin{pmatrix} \hat{\varepsilon}(\vec{k}) & -h_Q \hat{\sigma}^{(x)} \\ -h_Q \hat{\sigma}^{(x)} & \hat{\varepsilon}(\vec{k}_+) \end{pmatrix}, \quad (4)$$

with $\hat{\varepsilon}(\vec{k}) = \varepsilon(\vec{k}) \hat{\sigma}^{(0)} + \alpha \vec{g}(\vec{k}) \hat{\sigma}$ and $\vec{k}_+ = \vec{k} + \vec{Q}$. $\hat{G}^i(\vec{k}, i\omega_n)$ is a 2×2 matrix in spin space, $\omega_n = (2n+1)\pi T$ and T is the temperature.

We turn to the SC instability which we assume to arise through electron-electron interaction incorporated in the effective on-site repulsion U . The linearized Éliashberg equation is obtained in the standard procedure:

$$\lambda \Delta_{p,s_1,s_2}(\vec{k}) = - \sum_{\vec{k}', q, s_3, s_4} V_{p,q,s_1,s_2,s_3,s_4}(\vec{k}, \vec{k}') \psi_{q,s_3,s_4}(\vec{k}') \quad (5)$$

$$\psi_{p,s_1,s_2}(\vec{k}) = \sum_{i,j,s_3,s_4} \phi_{p,i,j,s_1,s_2,s_3,s_4}(\vec{k}) \Delta_{q,s_3,s_4}(\vec{k}'), \quad (6)$$

where $q = p$ ($q = 3-p$) for $i = j$ ($i \neq j$), $\vec{k}'' = \vec{k} + (i-1)\vec{Q}$ and

$$\begin{aligned} \phi_{p,i,j,s_1,s_2,s_3,s_4}(\vec{k}) &= T \sum_n G_{s_1,s_2}^i(\vec{k}, i\omega_n) \\ &\times G_{s_3,s_4}^j(-\vec{k} + (p-1)\vec{Q}, -i\omega_n) \quad (p = 1, 2). \end{aligned} \quad (7)$$

Here, we adopt the so-called weak coupling theory of superconductivity and ignore self-energy corrections and the frequency dependence of effective interaction.^{28,29} This simplification affects the resulting transition temperature but hardly the symmetry of pairing.²⁸ The effective interaction $V_{p,q,s_1,s_2,s_3,s_4}(\vec{k}, \vec{k}')$ originates from spin fluctuations which we describe within the RPA.²⁹

The linearized Éliashberg equation allows us to determine the form of the leading pairing instability which is attained for the temperature at which the largest eigenvalue λ in eq. (5) reaches unity. We perform the calculation at a given temperature, $T = 0.02$ and determine the most stable pairing state as the eigenfunction of the largest eigenvalue for the sake of numerical accuracy.²⁸ The typical value of the eigenvalue at $T = 0.02$ and $U = 4$ lies around $\lambda = 0.4 \sim 0.6$.

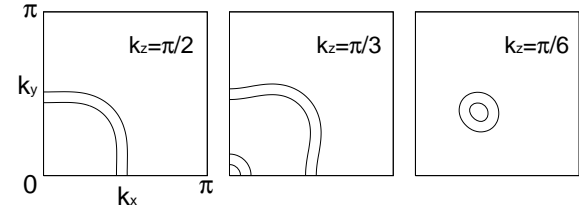


Fig. 1. The Fermi surfaces of the Hubbard model (eq. (1)) at $\alpha = 0.3$ and $h_Q = 0$. The cross sections at $k_z = \frac{\pi}{2}$, $k_z = \frac{\pi}{3}$ and $k_z = \frac{\pi}{6}$ are shown from the left to the right.

First of all, we discuss the symmetry of the SC state which we express by the following extended parameterization of the gap function:

$$\Delta_{1,s,s'}(\vec{k}) = \begin{pmatrix} -d_x(\vec{k}) + id_y(\vec{k}) & \Phi(\vec{k}) + d_z(\vec{k}) \\ -\Phi(\vec{k}) + d_z(\vec{k}) & d_x(\vec{k}) + id_y(\vec{k}) \end{pmatrix}, \quad (8)$$

where we use the usual even parity scalar function $\Phi(\vec{k})$ and the odd parity vector $\vec{d}(\vec{k})$. In the presence of AFM order a second component $\Delta_{2,s,s'}(\vec{k})$ appears. However, the basic properties and symmetries are little affected by $\Delta_{2,s,s'}(\vec{k})$. Within the described scheme we identify two stable solutions of the Éliashberg equation eqs. (5-7). One pairing state has dominant p -wave symmetry whose order parameter has the leading odd parity component $\vec{d}(\vec{k}) = (-\sin k_y, \beta \sin k_x, 0)$ and the admixed even parity part $\Phi(\vec{k}) = \cos k_x + \cos k_y$. The parameter β is unity in the absence of AFM order.

The other stable solution has dominantly d -wave character and can be viewed as an inter-layer pairing state: $\Phi(\vec{k}) = \{\sin k_x \sin k_z, \sin k_y \sin k_z\}$ (two-fold degenerate) admixed with odd-parity component $\vec{d}(\vec{k}) = \Phi(\vec{k})(\sin k_y, \sin k_x, 0)$. In the paramagnetic phase the most stable combination of the two degenerate states is chiral: $\Phi_{\pm}(\vec{k}) = (\sin k_x \pm i \sin k_y) \sin k_z$ which gains the maximal condensation energy in the weak-coupling approach. In the AFM state, however, the two states of $\Phi(\vec{k})$ are no longer degenerate.

A brief view on the pairing mechanism clarifies the origin of the stable pairing states. The static spin sus-

ceptibility is peaked around $\vec{Q} = (0, 0, \pi)$ consistent with the AFM order of the Ce moments. The in-plane ferromagnetic correlations favor the in-plane p -wave pairing. On the other hand, the interlayer AFM correlation drives interlayer spin singlet pairing. The stability of the two states is determined by the band filling n and the Coulomb repulsion U . Small U and large n favor the p -wave state, while the d -wave state is more stable for large U and small n . The two states are essentially degenerate for $U = 4$ and $n = 1.75$.

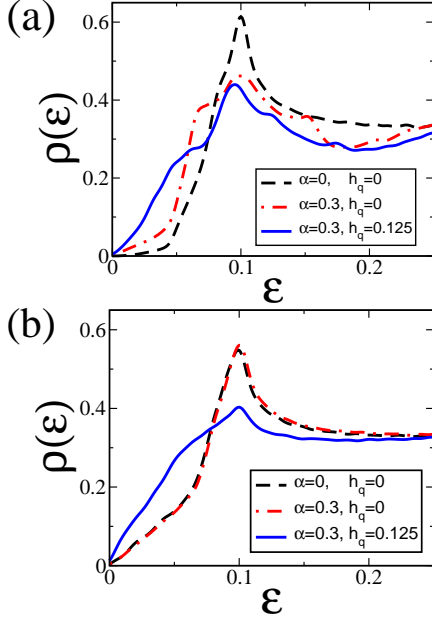


Fig. 2. (Color online) DOS $\rho(\varepsilon)$ for $U = 4$ in (a) dominantly p -wave state and (b) dominantly d -wave state. We show the results for $\varepsilon > 0$ because $\rho(\varepsilon)$ is particle-hole symmetric owing to its definition.

Next we turn to the influence of the AFM order on these pairing states. As a first point we discuss the quasi-particle DOS which is obtained by diagonalizing the 8×8 matrix,

$$\hat{H}_s(\vec{k}) = \begin{pmatrix} \hat{H}(\vec{k}) & -\hat{\Delta}(\vec{k}) \\ -\hat{\Delta}^\dagger(\vec{k}) & -\hat{H}(-\vec{k})^\top \end{pmatrix}, \quad (9)$$

where

$$\hat{\Delta}(\vec{k}) = \begin{pmatrix} \Delta_{1,s,s'}(\vec{k}) & \Delta_{2,s,s'}(\vec{k}) \\ \Delta_{2,s,s'}(\vec{k}_+) & \Delta_{1,s,s'}(\vec{k}_+) \end{pmatrix}. \quad (10)$$

The DOS is obtained by the eigenvalues as $\rho(\varepsilon) = \frac{1}{4N} \sum_{i,k} \delta(\varepsilon - E_i(\vec{k}))$. We determine the momentum and spin dependences of order parameter within the linearized Eliashberg equation at $T = 0.02$ and assume that those structures do not change below T_c . For our purpose it is not necessary to calculate the magnitude of the gap functions self-consistently as we are mainly interested on qualitative properties arising from the gap structure. Thus we choose the magnitude of the maximal gap, $\Delta_g = 0.1$, which may be large compared to the energy scales α or h_Q . However, we adopt this value for the

sake of numerical accuracy, having confirmed that lower values of Δ_g do not alter the result in a qualitative way.

We first consider the p -wave state (Fig. 2(a)). In the absence of ASOC and AFM order there are only point nodes along the $[001]$ -direction leading to a quadratic energy dependence of the DOS: $\rho(\varepsilon) = c_1 \varepsilon^2$. The inclusion of ASOC ($\alpha = 0.3$) yields two kinds of the line node. The admixture of the s -wave component is one cause of line nodes as discussed by Frigeri et al.¹⁰ The other origin of nodes lies in the specific structure of the g -vector. For the assumed band structure and g -vector, singularities of \vec{g} appear not only along the $[001]$ -direction (given by symmetry) but also accidentally on lines around $(k_x, k_y) = (\pm 0.4\pi, \pm 0.4\pi)$. The SC p -wave gap vanishes along the lines where $\vec{d}(\vec{k}) \perp \vec{g}(\vec{k})$.³⁰ This second type of line nodes, however, depends strongly on details of material parameters. Within our model the length of the line nodes arising from these mechanism are short leading only to a weak linear energy dependence of the DOS, $\rho(\varepsilon) = c_2 \varepsilon$ as can be seen in Fig. 2(a). The linear DOS increases remarkably through the AFM order (Fig. 2(a)), caused by two effects: (I) the Brillouin zone folding at $k_z = \pm\pi/2$; (II) the modification of SC order parameter. Effect (I) has been investigated by Fujimoto.¹⁴ It turns out that this effect is of minor quantitative importance, if $h_Q \ll W$ as in the present situation. Hence the main effect originates from (II), because the d_x - and d_y -components are no longer equivalent in the AFM state. The anisotropy parameter β in $\vec{d}(\vec{k}) = (-\sin k_y, \beta \sin k_x, 0)$ decreases with growing h_Q . In this way the SC gap becomes anisotropic leading to the extension of the line nodes and an even more pronounced linear energy dependence of the DOS. It should be noted that the line nodes discussed for this case are not symmetry protected but "accidental".

The d -wave state has already line nodes for symmetry reasons. In this case the low-energy DOS is not so strongly affected by the ASOC as shown in Fig. 2(b). But the slope increases, if the AFM order is included, since the pairing state changes its form from $d_{xz} \pm id_{yz}$ to d_{xz} . The latter has obviously more line nodes.

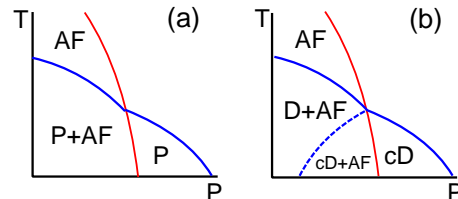


Fig. 3. (Color online) Schematic phase diagram in the P - T plane. (a) p -wave and (b) d -wave state. "D" ("cD") shows the d_{xz} -wave ($d_{xz} \pm id_{yz}$ -wave) state. The critical temperatures of SC and AFM orders are written so as to be consistent with the experiment.²⁶

Consequently, the low energy excitations are increased by the AFM order for both the p -wave and d -wave states. The resulting line node behavior is consistent with the experimental results at ambient pressure.¹⁷⁻¹⁹

The p -wave case leads to a simple phase diagram in the P - T plane (Fig. 3(a)). However, the situation is more intriguing for the d -wave case, since there is an additional phase transition line meeting at the crossing point of T_N and T_c . Generally we would expect an additional SC phase transition within the SC phase leading to chiral d -wave phase at low enough temperatures, while the SC high-temperature phase has only a finite d_{xz} -component (Fig. 3(b)). Although a second SC transition has been observed,³¹ it remains unclear whether it represents an intrinsic property or is caused by sample inhomogeneity.

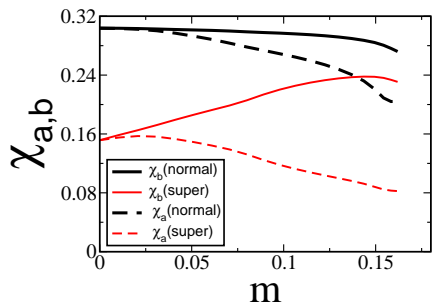


Fig. 4. (Color online) Magnetic susceptibility along the a - (dashed) and b -axis (solid) against the staggered spin polarization $m = | \langle \sum_{s,s'} \sigma_{ss'}^{(x)} c_{i,s}^\dagger c_{i,s'} \rangle |$. The thick and thin line show the results in the normal state and SC state at $T = 0$, respectively.

It has been reported that the Knight shift remains constant below T_c for any field direction.^{21,22} This result looks puzzling in view of calculations which suggest the decrease of spin susceptibility for fields in the ab -plane to the half of its normal state value.^{8-10,13} Here, we point out that this discrepancy can be resolved by taking into account the AFM order. The uniform spin susceptibility of the normal and SC states at $T = 0$ is shown in Fig. 4, assuming $T_c \ll \alpha$. No correlation effects have been taken into account here. For fields $H \perp h_Q$ the normal state and SC state susceptibility merge for increasing staggered moment. On the other hand, for $H \parallel h_Q$ the behavior is opposite. Assuming that the anisotropy energy is sufficiently small, the condition $H \perp h_Q$ is generally favored. Together with other effects such as vortex scattering and the formation of a helical SC phase¹² the influence of AFM order could eventually account for the experimental results.^{21,22} Note that Fig. 4 is obtained without taking into account the canting of AFM moment in contrast to Ref. 15 where the AFM coupling to the local moment is assumed to explain a similar property. Another mechanism to enhance the spin susceptibility below T_c has been proposed by Fujimoto, which is based on a strong particle-hole asymmetry.¹⁴ However the β -band in our model eq. (1) does not satisfy the necessary conditions. If the AFM order is the main cause for the behavior of the spin susceptibility for in-plane fields, a distinct change should be observed when the AFM order is suppressed by pressure.

In summary, we have examined various aspects of the pairing state in CePt₃Si based on a Hubbard model in-

cluding the ASOC and AFM order. For this purpose we chose the β -band of CePt₃Si, and found based on spin fluctuation mediated pairing interaction that the in-plane p -wave and inter-plane d -wave states are most likely candidates. Both states show line node behavior, consistent with experiments at ambient pressure.¹⁷⁻¹⁹ The AFM order plays an important role in various respects: (I) the SC gap structure is remarkably deformed through the AFM staggered moment. (II) The AFM order can give rise to multiple SC phase transitions. (III) The in-plane magnetic susceptibility in the SC state can be increased giving an explanation for the Knight shift measurements.^{21,22} The p -wave state is more likely realized in CePt₃Si because it can explain the coherence peak in the NMR $1/T_1T$.^{11,14,20} Finally, our results suggest that the investigation of the SC phase under the pressure would be interesting, in order to explore the SC phase in the regime where AFM order does no longer exist.

The authors are grateful to D. F. Agterberg, S. Fujimoto, J. Flouquet, N. Hayashi, K. Izawa, Y. Matsuda, V. P. Mineev, H. Mukuda, T. Shibauchi, R. Settai, H. Tanaka, T. Tateiwa and M. E. Zhitomirsky for fruitful discussions. This study has been supported by the Nishina Memorial Foundation, the Swiss Nationalfonds and the NCCR MaNEP. Numerical computation was carried out at the Yukawa Institute Computer Facility.

- 1) E. Bauer *et al.*: Phys. Rev. Lett **92** (2004) 027003; J. Low. Temp. Phys. **31** (2005) 748.
- 2) T. Akazawa *et al.*: J. Phys. Soc. Jpn. **73** (2004) 3129.
- 3) N. Kimura *et al.*: Phys. Rev. Lett. **95** (2005) 247004.
- 4) I. Sugitani *et al.*: J. Phys. Soc. Jpn. **75** (2006) 043703.
- 5) R. Settai: private communication.
- 6) K. Togano *et al.*: Phys. Rev. Lett. **93** (2004) 247004;
- 7) T. Shibauchi *et al.*: Phys. Rev. B **74** (2006) 220506.
- 8) V. M. Edelstein: Sov. Phys. JETP **68** (1989) 1244; Phys. Rev. Lett **75** (1995) 2004; Phys. Rev. B **72** (2005) 172501.
- 9) L. P. Gor'kov and E. I. Rashba: Phys. Rev. Lett **87** (2001) 037004.
- 10) P. A. Frigeri *et al.*: Phys. Rev. Lett **92** (2004) 097001; New. J. Phys. **6** (2004) 115; cond-mat/0505108.
- 11) N. Hayashi *et al.*: Phys. Rev. B **73** (2006) 024504; 092508.
- 12) R. P. Kaur *et al.*: Phys. Rev. Lett **94** (2005) 137002.
- 13) K. V. Samokhin: Phys. Rev. B **70** (2004) 104521; **72** (2005) 054514; Phys. Rev. Lett **94** (2005) 027004; V. P. Mineev and K. V. Samokhin: cond-mat/0612546.
- 14) S. Fujimoto: Phys. Rev. B **74** (2005) 024515; J. Phys. Soc. Jpn. **75** (2006) 083704; cond-mat/0605290.
- 15) H. Shimahara: Phys. Rev. B **72** (2005) 134518.
- 16) N. Metoki *et al.*: J. Phys. Condens. Matter **16** (2004) L207.
- 17) K. Izawa *et al.*: Phys. Rev. Lett **94** (2005) 197002.
- 18) I. Bonalde *et al.*: Phys. Rev. Lett **94** (2005) 207002.
- 19) T. Takeuchi *et al.*: J. Phys. Soc. Jpn. **76** (2007) 014702.
- 20) M. Yogi *et al.*: Phys. Rev. Lett **93** (2004) 027003.
- 21) M. Yogi *et al.*: J. Phys. Soc. Jpn. **75** (2006) 013709.
- 22) W. Higemoto *et al.*: J. Phys. Soc. Jpn. **75** (2006) 124713.
- 23) K. V. Samokhin *et al.*: Phys. Rev. B **69** (2004) 094514.
- 24) S. Hashimoto *et al.*: J. Phys. Condens. Matter **16** (2004) L287.
- 25) A. Kozhevnikov and V. Anisimov: private communication.
- 26) T. Tateiwa *et al.*: J. Phys. Soc. Jpn. **74** (2005) 1903.
- 27) For a review, Y. Kitaoka *et al.* J. Phys. Soc. Jpn. **74** (2005) 186; J. Flouquet *et al.*: cond-mat/0505713.
- 28) Y. Yanase *et al.*: Phys. Rep. **387** (2004) 1.
- 29) K. Miyake *et al.*: Phys. Rev. B **34** (1986) 6554; D. J. Scalapino *et al.*: Phys. Rev. B **34** (1986) 8190.

30) Y. Yanase and M. Sigrist: in preparation.

31) K. Nakatsuji *et al.*: J. Phys. Soc. Jpn. **75** (2006) 084717.